Quantum-Based Atomistic Simulation of Metals at Extreme Conditions

J. A. Moriarty, J. N. Glosli, R. Q. Hood, J. E. Klepeis, D. A. Orlikowski, P. Soderlind, L. H. Yang

January 16, 2008

LAWRENCE LIVERMORE NATIONAL LABORATORY

Disclaimer

This document was prepared as an account of work sponsored by an agency of the United States government. Neither the United States government nor Lawrence Livermore National Security, LLC, nor any of their employees makes any warranty, expressed or implied, or assumes any legal liability or responsibility for the accuracy, completeness, or usefulness of any information, apparatus, product, or process disclosed, or represents that its use would not infringe privately owned rights. Reference herein to any specific commercial product, process, or service by trade name, trademark, manufacturer, or otherwise does not necessarily constitute or imply its endorsement, recommendation, or favoring by the United States government or Lawrence Livermore National Security, LLC. The views and opinions of authors expressed herein do not necessarily state or reflect those of the United States government or Lawrence Livermore National Security, LLC, and shall not be used for advertising or product endorsement purposes.

QUANTUM-BASED ATOMISTIC SIMULATION OF METALS AT EXTREME CONDITIONS

John A. Moriarty, James N. Glosli, Randolph Q. Hood, John E. Klepeis, Daniel A. Orlikowski, Per Söderlind, and Lin H. Yang

Lawrence Livermore National Laboratory, Livermore, CA 94551

Keywords: Atomistic simulation, MGPT potentials, phase transitions, melting, strength

Abstract

First-principles generalized pseudopotential theory (GPT) provides a fundamental basis for bridging the quantum-atomistic gap from density-functional quantum mechanics to large scale atomistic simulation in metals and alloys. In directionally-bonded bcc transition metals, advanced generation *model* GPT or MGPT potentials based on canonical *d* bands have been developed for Ta, Mo and V and successfully applied to a wide range of thermodynamic and mechanical properties at both ambient and extreme conditions of pressure and temperature, including high-pressure phase transitions, multiphase equation of state; melting and solidification; thermoelasticity; and the atomistic simulation of point defects, dislocations and grain boundaries needed for the multiscale modeling of plasticity and strength. Recent algorithm improvements have also allowed an MGPT implementation beyond canonical bands to achieve increased accuracy, extension to *f*-electron actinide metals, and high computational speed. A further advance in progress is the development temperature-dependent MGPT potentials that subsume electron-thermal contributions to high-temperature properties.

Introduction

Accurate and predictive large-scale atomistic simulation of materials properties is a forefront challenge in condensed-matter and materials physics. There currently exists a wide spectrum of atomic-scale calculational methods, extending from exact quantum-mechanical techniques to classical descriptions with totally empirical force laws. All of these methods fall into one of two distinct categories separated by a material-dependent gap. On one side of this gap are electronic-structure methods based on direct quantum-mechanical treatments. These include *quantum simulations* that attempt to treat electron and ion motion on an equal footing, solving on the fly for both the electronic states of the system and the forces on the individual ions. In most metals and alloys, methods based on modern density-functional theory (DFT) [1] can provide a highly accurate description of the system and are chemically very robust, but they come at the price of being severely limited in the size ($\leq$1000 atoms) and duration ($\leq$10 ps) of the simulation. On the other side of the gap are methods used in *atomistic simulations*, such as molecular dynamics (MD), that treat only the ion motion, allowing much larger ($\sim 10^8$-10^{10} atoms) and longer ($\sim$100 ns) simulations by solving classical Newtonian equations of motion with the forces derived from explicit interatomic potentials. Bridging the *electronic-atomistic gap* is possible through the development of first-principles *quantum-based potentials* based on a systematic coarse-graining of the DFT electronic structure. In this paper, we present a brief overview of recent work at LLNL on developing quantum-based interatomic potentials for *d*-bonded transition metals from density-functional theory and widely applying these potentials to the atomistic simulation of materials properties at both ambient and extreme conditions.

Quantum-Based Potentials

Within DFT quantum mechanics, first-principles generalized pseudopotential theory (GPT) provides a fundamental basis for *ab initio* interatomic potentials in metals and alloys. In the GPT applied to transition metals [2], a mixed basis of plane waves and localized *d*-state orbitals is used to self-consistently expand the electron density and total energy of the system in terms of weak *sp* pseudopotential, *d-d* tight-binding, and *sp-d* hybridization matrix elements, which in turn are all directly calculable from first principles. For a bulk transition metal, one obtains the real-space total-energy functional

$$E_{tot}(R_1 \ldots R_N) = NE_{vol}(\Omega) + \frac{1}{2}\sum_{i,j}{}' v_2(ij;\Omega) + \frac{1}{6}\sum_{i,j,k}{}' v_3(ijk;\Omega) + \frac{1}{24}\sum_{i,j,k,l}{}' v_4(ijkl;\Omega) \qquad (1)$$

The leading volume term in this expansion, E_{vol}, as well as the two-, three-, and four-ion interatomic potentials, v_2, v_3 and v_4, are volume dependent, *but structure independent* quantities and thus *transferable* to arbitrary bulk ion configurations. The angular-force multi-ion potentials v_3 and v_4 reflect directional-bonding contributions from partially-filled *d* bands and are important for mid-period transition metals. In the full *ab initio* GPT, however, these potentials are multi-dimensional functions, so that v_3 and v_4 cannot be readily tabulated for application purposes. This has led to the development of a simplified *model* GPT or MGPT, which achieves short-ranged, analytic potential forms that can be applied to large-scale atomistic simulations [3-6].

The MGPT is derived from the GPT through a series of systematic approximations applicable to central transition metals. Canonical *d* bands are introduced to express the *d*-state components of v_2 and the multi-ion potentials v_3 and v_4 analytically in terms of a single radial function and three universal angular functions that depend only on *d* symmetry and apply to all transition metals and all volumes. To compensate for the approximations introduced into the MGPT, the *d*-state potential coefficients in v_2, v_3 and v_4 together with E_{vol} are constrained by fundamental theoretical and/or experimental data. In our current preferred scheme for bcc metals, we fit a combination of first-principles DFT calculations and experimental data on the cold equation of state, shear elastic moduli, unrelaxed vacancy formation energy and Debye temperature over a prescribed volume or pressure range. Advanced generation MGPT potentials have been so obtained in Ta to 1000 GPa [4,5], in Mo to 400 GPa [6,7] and in V to 230 GPa [7]. Representative results for these three metals are displayed in Fig. 1 at their respective equilibrium volumes.
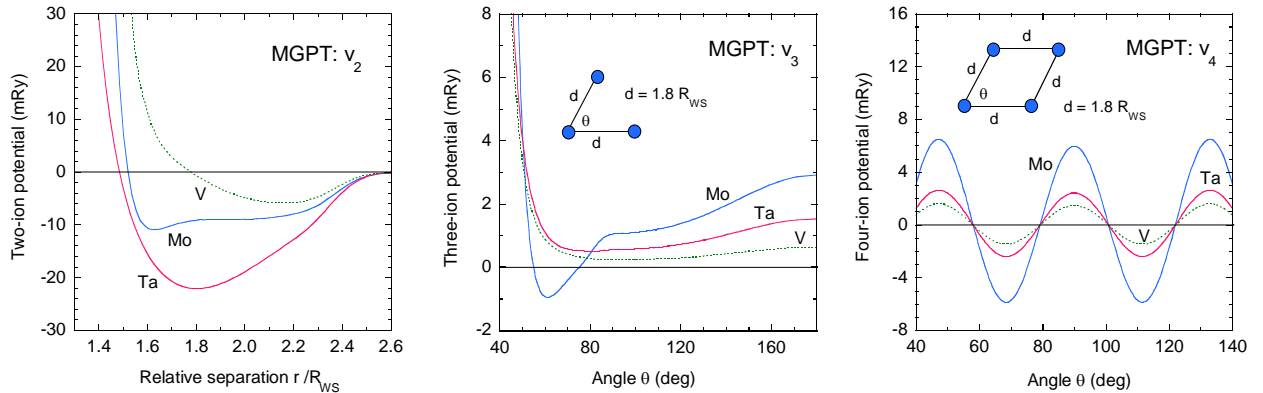

Figure 1. Present advanced generation MGPT multi-ion potentials v_2, v_3 and v_4 for Ta, Mo and V calculated at their respective equilibrium volumes.

Selected Applications

The MGPT potentials for Ta, Mo and V have been applied to a wide range of structural, thermodynamic, defect and mechanical properties at both ambient and extreme conditions. These properties include structural phase stability and high-pressure phase transitions; multiphase equation of state, melting and rapid solidification; high-pressure elastic moduli and ideal strength; thermoelasticity and sound velocities; vacancy and self-interstitial formation and migration; grain-boundary structure; dislocation core structure and mobility; and the multiscale modeling of yield strength. Here we consider a few selected applications of current high interest.

Structural Phase Stability and High-Pressure Phase Transitions

Although our transition-metal MGPT potentials are constrained by single-phase bcc data, they retain a high degree of the structural transferability inherent in the full GPT, so that phase stability and high-pressure phase transitions are generally well described without further constraint. The overall structural trends in the central transition metals are controlled by d-band filling and the well known $s \rightarrow d$ transition at high pressure. This accounts for the characteristic bcc structure in the Group VB and VIB metals, a corresponding large fcc-bcc energy difference, and an eventual bcc $\rightarrow$ hcp transition predicted in the VIB metals at ultra-high pressures [8]. Within the MGPT, about half of the fcc-bcc energy arises from the oscillatory four-ion potential v_4 and the transition to hcp is associated with v_4 changing sign under high pressure.

In addition to these overall trends, there are interesting observed secondary structural trends in these metals that are also well captured by the MGPT potentials. The first of these is a relatively small A15-bcc energy difference that results in a competitive and metastable A15 structure at low pressure in the heavy $5d$ metals Ta and W. This competition is very keen in Ta near melt and has been is seen in MD/MGPT simulations of the solidification process [4]. The second trend is associated with a Fermi-surface driven anomaly in the C_{44} elastic constant of bcc Group VB metals that occurs over a material-dependent range of pressure [9]. This accounts for the well known small magnitude of C_{44} in Nb near ambient pressure, while in V this modulus actually becomes negative at high pressure resulting in a phase transition to a rhombohedral structure. The bcc $\rightarrow$ rhom transition has recently been observed in diamond-anvil-cell (DAC) experiments at 69 GPa [10] and confirmed in detail by DFT electronic-structure calculations [11]. Our current MGPT potentials for V also fully capture this behavior, as shown in Fig. 2.
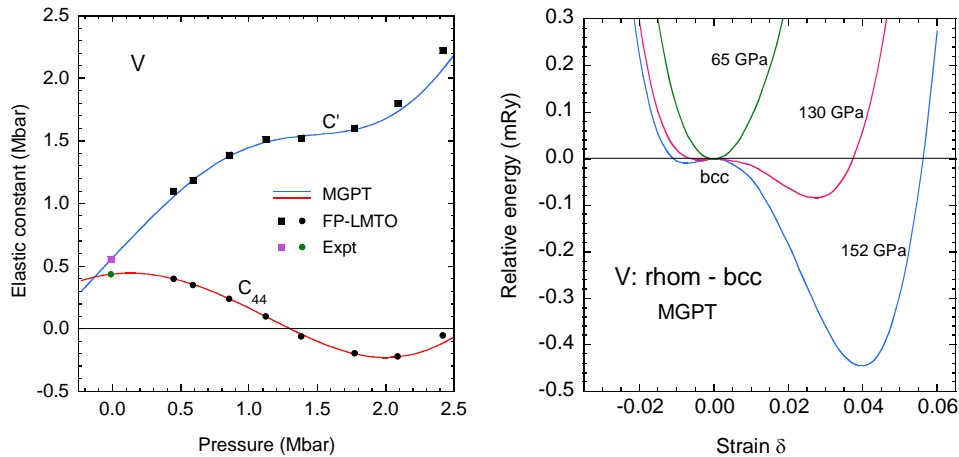

Figure 2. MGPT shear elastic moduli and rhom-bcc energy difference under pressure in V.

Multiphase Equation of State and Melt

We next discuss the quantum-based calculation of finite temperature thermodynamics properties, with emphasis on the multiphase equation of state (EOS) and melting curve of Ta. We treat the observed bcc solid, the liquid and the metastable A15 phase and break all thermodynamic quantities into cold (zero-temperature), ion-thermal and electron-thermal contributions. The cold bcc component of our Ta EOS is constrained by DFT electronic-structure calculations in the 0-1000 GPa pressure range [12], while the ion-thermal EOS components are calculated from the corresponding MGPT potentials using quasiharmonic lattice dynamics in the low-T solid and MD simulation in the high-T solid and in the liquid. Good quality bcc phonons are obtained and these yield a Grüneisen parameter with a nonlinear volume dependence at high pressure. The remaining electron-thermal EOS components are obtained by using MD/MGPT snapshots of finite-T structure in small-cell DFT calculations and then configuration averaging. Although the competitive nature of the A15 structure is observed, bcc is the predicted solid phase over the entire 0-1000 GPa range from T=0 to melt. A two-phase bcc-liquid EOS and melt curve have been calculated over this pressure range and a temperature range of 0-35,000 K [4]. The calculated 300-K isotherm and principal Hugoniot agree well with DAC and shock-compression experimental data, respectively. Our most recent calculated melt curve obtained from new highly accurate bcc and liquid free energies [7] is displayed in the left panel of Fig. 3 and compared against isobaric expansion data [13], the observed shock melting point [14] and laser-heated DAC measurements [15]. High-pressure melting in transition metals has become controversial with unexpectedly flat transition-metal melt curves recently obtained in the DAC experiments. In contrast, we predict a steep melting curve for Ta, which is consistent with all of the dynamic data. Moreover, as shown in right panel of Fig. 3, our calculated sound velocities [16] in bcc and liquid Ta are in good agreement with those measured along the Hugoniot in the shock melting experiments, confirming the interpretation of those experiments.
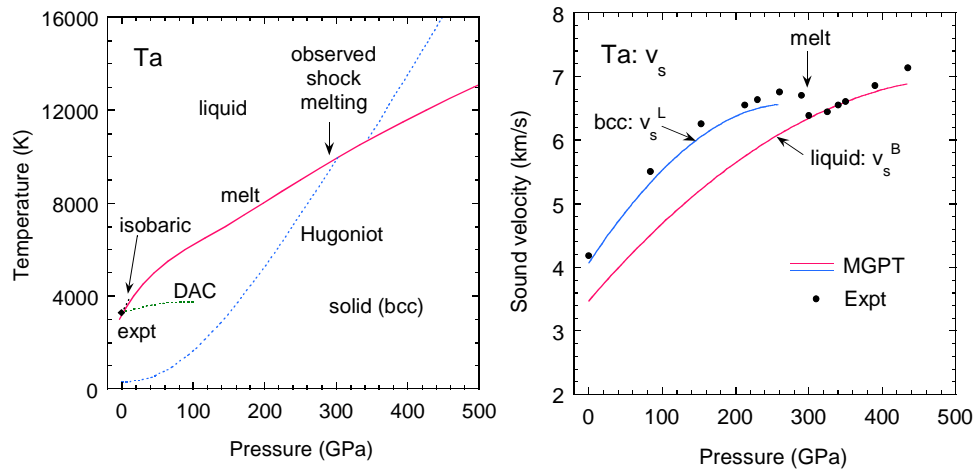

Figure 3. Left panel: calculated Ta melt curve and Hugoniot compared with experimental data [13-15]; right panel: calculated [16] and measured [14] bcc and liquid Ta sound velocities.

Dislocations and the Multiscale Modeling of Yield Stress

The low-T and high-strain-rate plastic behavior of bcc transition metals is controlled by the intrinsic core properties of $a/2\langle 111\rangle$ screw dislocations. Unlike the highly mobile edge dislocations in these metals, the motion of the screw dislocations is severely restricted by the

non-planar atomic structure of its core, resulting in low mobility, thermal activated kink pairs and a temperature-dependent yield stress. For the accurate atomistic simulation of dislocation core properties, we have developed an advanced Green's function (GF) simulation method that allows both static and dynamic calculations [5]. Extensive GF/MGPT simulations have been carried out in Ta and Mo over wide ranges of pressure on the core structure, the Peierls stress τ_P and its stress-orientation dependence, and kink-pair energetics of $a/2\langle 111\rangle$ screw dislocations [5,6]. In general, the core structure exhibits a three-fold directional spreading, of variable magnitude or polarization. We predict an isotropic core structure for Mo and Ta near equilibrium and into expansion, but an increasingly polarized core under hydrostatic pressure.

Similarly, our calculated τ_P in Ta and Mo exhibits a strong dependence on the orientation of the applied stress and large deviations from the well-known Schmid law. Our minimum calculated τ_P in Mo at ambient pressure is close to the corresponding experimental estimate based on extrapolating the observed yield stress to zero temperature, and is a major improvement over that previously obtained with earlier generation MGPT potentials [6]. In Ta and Mo we also find that both the ideal shear strength of the bcc perfect crystal and τ_P display approximate linear scaling with the $\langle 111\rangle$ shear modulus $G_{111} = (2C' + C_{44})/3$ to 1000 and 400 GPa, respectively. These findings support the linear scaling of yield strength with shear modulus, as is assumed in most of the current constitutive models used in the high-pressure materials community.

At finite temperature, the motion of the bcc screw dislocations occurs by the thermally assisted formation and migration of kink pairs. In microscale dislocation dynamics (DD) simulations of single-crystal plasticity for bcc metals [17], a key input quantity is the stress-dependent activation enthalpy for kink-pair formation, $\Delta H(\tau)$, which controls the dislocation mobility through the stress-dependent velocity of a screw dislocation. We have performed extensive GF/MGPT atomistic simulations of $\Delta H(\tau)$ for both Ta and Mo over a wide range of pressures. These results have then been fitted to the analytic form used in the DD simulations. One can thereby import the required atomistic information directly into DD simulations for real materials at any assumed pressure condition. Such atomistically-informed DD simulations of yield stress as a function of temperature have recently been performed at selected pressures in both Ta and Mo [6,18].

Recent Advances Beyond the Standard Theory

One of the advantages of the first-principles GPT formalism for interatomic potentials is that it is systematically improvable in a manner consistent with quantum mechanics. Recently, we have made major strides in this direction by developing a more general matrix MGPT representation. In the matrix MGPT, the three- and four-ion angular functions are recast as matrix products that can be evaluated on the fly numerically during a simulation. In this representation, several major extensions of the standard MGPT are possible. First, the theory can be immediately generalized to treat non-canonical d-bands with arbitrary tight-binding coefficients. Second, one may further generalize from d states to f states to treat actinide metals by replacing 5×5 d-state matrices with 7×7 f-state ones.

A third major advance that has been facilitated by the matrix MGPT is algorithm improvements in the evaluation of energies and forces, most notably an optimized strategy to calculate the multi-ion energy terms in Eq. (1) and an explicit analytic treatment of the forces [19]. This has

resulted in MGPT simulation codes that are an order of magnitude faster and has dramatically increased the size and scope of problems that can be addressed on large parallel platforms. The most striking example of this is the recent large-scale MD/MGPT simulations of rapid soldification of Ta that have been performed on LLNL's new BlueGene/L supercomputer [20].

Two other important areas we are currently pursuing are the use of non-canonical bands and the development of temperature-dependent MGPT potentials. In principle, non-canonical bands permit a more accurate characterization of the underlying electronic structure. In practice, we have found them useful in improving the overall quality of the calculated phonon spectrum in certain difficult cases such as Mo. Interestingly, the introduction of just two non-canonical band parameters seems to be able to improve *all* phonons at *all* volumes. The concept of temperature-dependent potentials for *d*- and *f*-electron metals is an important one because of the large electron-thermal effects at temperatures as low as melt. These effects are normally treated separtely from the normal ion-thermal effects, but we are now trying to capture them simultaneously and self-consistently by building MGPT potentials on the basis of the total electron free energy at finite temperature.

Acknowledgment

References

1. W. Kohn, and L. J. Sham, *Phys. Rev.* **140**, A1133 (1965).
2. J. A. Moriarty, *Phys. Rev. B* **38**, 3199 (1988).
3. J. A. Moriarty, *Phys. Rev. B* **42**, 1609 (1990) and **49**, 12431 (1994).
4. J. A. Moriarty *et al.*, *J. Phys.: Condens. Matter* **14**, 2825 (2002).
5. L. Yang, P. Söderlind, and J. A. Moriarty, *Philos. Mag. A* **81**, 1355 (2001).
6. J. A. Moriarty *et al.*, *J. Mater. Research* **21**, 563 (2006).
7. J. A. Moriarty, unpublished.
8. J. A. Moriarty, *Phys. Rev. B* **45**, 2004 (1992).
9. A. Landa *et al.*, *J. Phys.: Condens. Matter* **18**, 5079 (2006) and *J. Phys. Chem. Solids* **67**, 2056 (2006).
10. Y. Ding *et al.*, *Phys. Rev. Lett.* **98**, 85502 (2007).
11. B. Lee *et al.*, *Phys. Rev. B* **75**, 180101 (2007).
12. P. Söderlind and J. A. Moriarty, *Phys. Rev. B* **57** 10340 (1998).
13. J. W. Shaner, G. R.Gathers, and C. Minichino, *High Temp.-High Pressures* **9**, 331 (1977).
14. J. M. Brown, and J. W. Shaner, *Shock Waves in Condensed Matter 1983* (Elsevier, Amsterdam, 1984), p. 91.
15. D. Errandonea *et al.*, *Phys. Rev. B* **63**, 132104 (2001) and *J. Phys.: Condens. Matter* **15**, 7635 (2003).
16. D. A. Orlikowski, P. Söderlind, and J. A. Moriarty *Phys. Rev. B* **74**, 54109 (2006).
17. M. Tang, L. P. Kubin, and G. R. Canova, *Acta mater.* **46**, 3221 (1998).
18. M. Tang, unpublished.
19. J. N. Glosli, unpublished.
20. F. H. Streitz, J. N. Glosli, and M. V. Patel, *Phys Rev. Lett.* **96**, 225701 (2006).